Optica Applicata, Vol. XL, No. 1, 2010

Structural, electrical and optical properties of AZO/SiO$_2$/*p*-Si SIS heterojunction prepared by magnetron sputtering

HeBo[1], ZhongQuanMa[1], XuJing[2], ZhaoLei[1], ZhangNanSheng[1], LiFeng[1], ShenCheng[1], ShenLing[1], MengXiaJie[1], ZhouChengYue[1], YuZhengShan[1], YinYanTing[1]

[1]SHU-Solar E PV Laboratory, Department of Physics, Shanghai University, Shanghai 200444, China

[2]State Key Laboratory of Advanced Technology for Materials Synthesis and Processing,
WuHan University of Technology, HuBei WuHan 430070, China

ZnO thin films doped with aluminum (AZO) were deposited on silicon dioxide covered type texturized Si substrates by radio frequency magnetron sputtering, to fabricate AZO/SiO$_2$/*p*-Si heterojunction, as an absorber for ultraviolet cell. The microstructure, optical and electrical properties of the Al-doped ZnO films were characterized by XRD, SEM, UV-VIS spectrophotometer, current–voltage measurement, and four point probe technique, respectively. The results show that AZO films are of good quality. The electrical junction properties were investigated by I–V measurement, which reveals that the heterojunction shows rectifying behavior under a dark condition. The ideality factor and the saturation current of this diode are 24.42 and 8.92×10^{-5} A, respectively. And the values of I_F/I_R (I_F and I_R stand for forward and reverse current, respectively) at 10 V are found to be as high as 38. It shows fairly good rectifying behavior indicating formation of a diode between AZO and *p*-Si.

Keywords: Al-doped ZnO (AZO), sputtering, SIS heterojunction, current–voltage (I–V) characteristics.

1. Introduction

As shown in previous work, semiconductor–insulator–semiconductor (SIS) diodes have certain features which make them more attractive for solar energy conversion than conventional Shottky, MIS, or other heterojunction structures [1]. For example, efficient SIS solar cell such as indium tin oxide (ITO) on silicon have been reported, where the crystal structures and the lattice parameters of Si (diamond, $a = 0.5431$ nm), SnO$_2$ (tetragonal, $a = 0.4737$ nm, $c = 0.3185$ nm), In$_2$O$_3$ (cubic, $a = 1.0118$ nm) show that they are not particularly compatible and thus not likely to form good devices. However, the SIS structure is potentially more stable and theoretically more efficient than either a Schottky or a MIS structure. The origins of this potential superiority are the suppression of majority-carrier tunneling in the high potential barrier region of SIS structure, and the existence of a thin interface layer which minimizes the amount and impact of interface states. This results in an extensive choice of the heterojunction partner with a matching band gap in the front layer. In addition, the top semiconductor film can serve as an antireflection coating [2], a low-resistance window, as well as the collector of the $p-n$ junction.

Furthermore, the semiconductor with a wide-band gap as the top layer of SIS structure can eliminate the surface dead layer which often occurs within the homojunction devices. On the other side, this absence of the light absorption of visible region in a surface layer can improve the ultraviolet response of the internal quantum efficiency. Among many transparent conductive oxides (TCO) of transition metals, ZnO:Al is one of the best *n*-type semiconductor layers. It has low resistivity, high transmittance, optimized surface texture for light trapping, and big band gap of $E_g \approx 3.3$ eV [3].

ZnO is an *n*-type wide-band gap semiconductor with a hexagonal wurtzite structure [4]. It has been prepared by various deposition techniques, such as sputtering, sol−gel process, spray pyrolysis, pulsed laser deposition, chemical vapour deposition (CVD), *etc*. The sputtering technique allows uniform films to be obtained with good orientation on different substrates at a moderate deposition temperature.

ZnO/Si heterojunctions are of particular interest in the integration of optoelectronic devices utilizing the hybrid advantages of the large exaction binding energy of the ZnO thin film and the cheapness of Si substrates. However, there are a few reports on the *n*-ZnO/*p*-Si heterojunction where the ZnO film is grown by different techniques. For example, Ajimsha reported the electrical characteristics of *n*-ZnO/*p*-Si heterojunction diodes grown by pulsed laser deposition at different oxygen pressures [5]. Basu prepared ZnO/*p*-Si junction by CVD and reported an ideality factor of 2.57 [6]. Kumar studied the characterization of sol−gel derived yttrium-doped *n*-ZnO/*p*-Si heterostructure [7]. Sun achieved UV electroluminescence (EL) emission from ZnO nanorods with *n*-ZnO/*p*-Si heterojunction structure fabricated by the hydrothermal method [8].

Thus, the present paper is based on a study to use a polycrystalline AZO film deposited by radio-frequency (RF) magnetron sputtering on the ultrathin SiO_2/*p*-Si substrate as a photon window for photoelectric device as well as a semiconducting layer which creates a depletion region and build-in potential in produced heterojunction.

2. Experiment

For the purpose of fabricating SIS structure, *p*-type texturized Si wafers with a boron--doping concentration ($\sim 7.2\times10^{15}$ cm^{-3}) corresponding to 2 Ωcm were used as the substrates of the heterojunction. The wafers were prepared by a standard cleaning procedure, then they were dipped in 10% HF solution for one minute to remove the native oxide layer. Finally, the wafers were dried in a flow of nitrogen.

By thermal evaporation, 1 μm-thick Al electrode was deposited on the back side. Then the samples were annealed at 500 °C for 20 min in N_2:O_2 = 4:1 condition to form good ohmic contact and an ultrathin oxide layer (about 15–20 Å) was grown on the *p*-Si surface.

The Al doped ZnO films were deposited on the oxidized silicon substrates in a RF magnetron sputtering system. The target was a sintered ceramic disk of ZnO doped with 2 wt% Al_2O_3 (purity 99.99%). The base pressure inside the chamber was pumped down to less than 5×10^{-4} Pa. Sputtering was carried out at a working gas (pure Ar) pressure of 1 Pa. The Ar flow ratio was 30 sccm. The RF power and the temperature on substrates were kept at 100 W and 300 °C, respectively. The sputtering was proceeded for 2.5 hours. The junction area is 2×2 cm^2.

Finally, by DC sputtering, a 1 μm Al metal film was deposited with a shadow mask on the AZO surface for the top electrode. The area of the Al electrode is 1×1 mm^2. Figures 1 and 2 show the schematic and bandgap structure of the novel AZO/SiO_2/*p*-Si SIS heterojunction device [9].

The thickness of AZO film was measured by a step profiler. The microstructure of the films was characterized by XRD and SEM. The optical transmission of the films was measured by UV-VIS spectrophotometer. The electrical properties of Al-doped

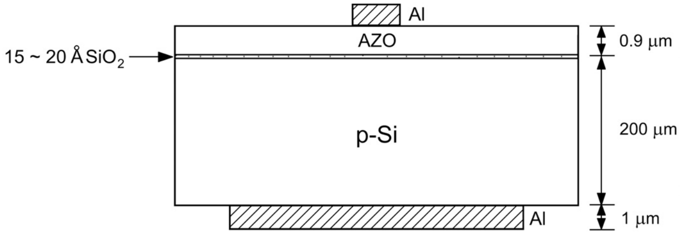

Fig. 1. The structure of AZO/SiO_2/*p*-Si heterojunction.

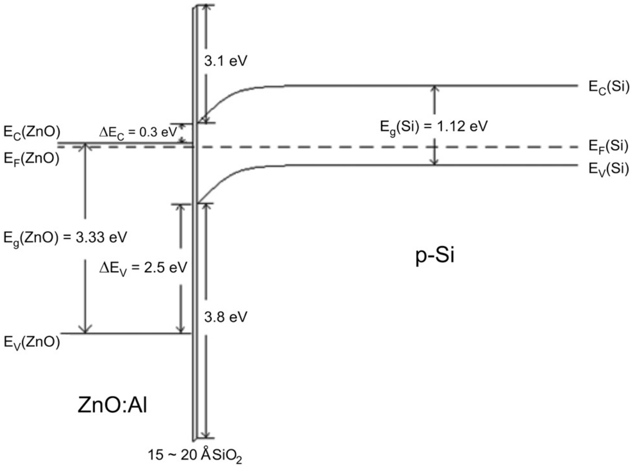

Fig. 2. Bandgap structure of the novel AZO/SiO_2/*p*-Si heterojunction.

ZnO films were characterized by four point probe. The current–voltage characteristics of the device was measured by Agilent 4155C semiconductor parameter analyzer (with probe station, the point of a probe is 5 μm).

3. Results and discussion

3.1. Microstructure, optical and electric properties of AZO films

Figure 3 shows the XRD spectra of AZO film on glass, which was deposited by RF magnetron sputtering. The dominant peak located at 34.4° is attributed to the ZnO (002) diffraction. The results indicate that the film has a hexagonal wurtzite structure with its dominant orientation along the *c*-axis perpendicular to the substrate surface.

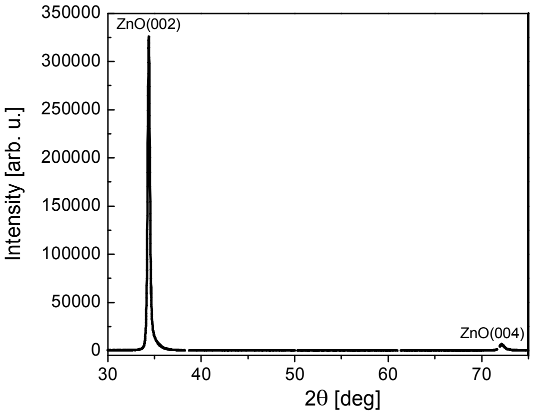

Fig. 3. XRD spectra of the Al-doped ZnO on glass.

In order to obtain more structural information and evaluate the mean grain size *D* of the films, we adopted the Scherrer formula [10]:

$$D = \frac{0.9\lambda}{\beta\cos\theta} \tag{1}$$

where λ, θ, β were X-ray wavelength (1.54056 Å), the Bragg diffraction angle, and the FWHM of AZO(002) diffraction peak, respectively. The full width at half maximum (FWHM) of the (002) ZnO peak observed in the X-ray diffraction spectra was as narrow as 0.3°, implying that the grown films had a very high degree of crystallinity. The mean grain size of the film was 32 nm.

Figure 4 shows the SEM image of the Al-doped ZnO film deposited by RF magnetron sputtering on glass. It can be easily seen that the grains are tightly packed.

In order to learn the optical absorption and energy band structure of AZO films, the transmission spectrum of the Al doped ZnO film deposited on the glass substrate (sputtering time is 1 hour) was measured (see Fig. 5). The thickness of AZO film is about 3560 Å. The average transmittance of the film is about 90% in the visible region.

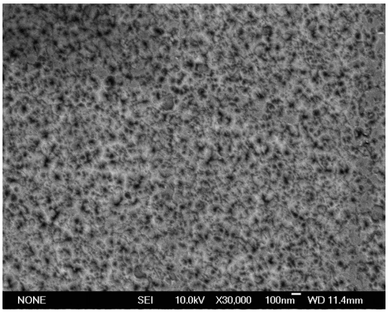

Fig. 4. The SEM micrographs of ZnO:Al film deposited by RF magnetron sputtering on glass.

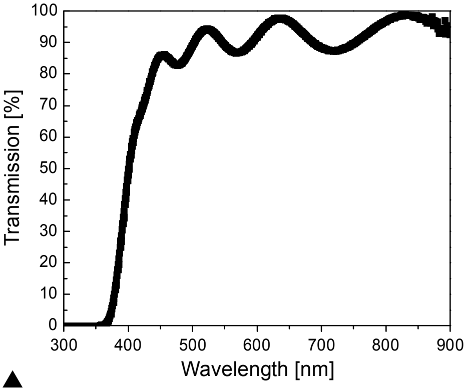

▲

Fig. 5. Transmission spectra of the AZO film.

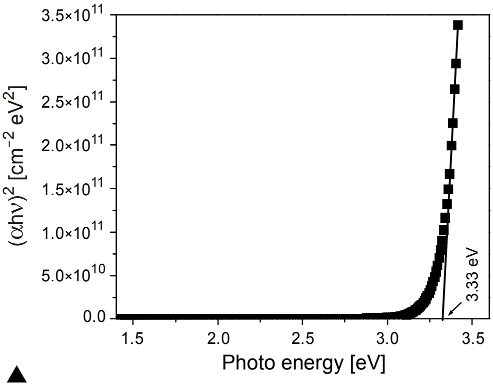

▲

Fig. 6. Variation of $(\alpha h\nu)^2$ vs. $h\nu$ of AZO film.

The absorption coefficient α was evaluated from the measurements of optical transmittance T according to the following relation [10]:

$$\alpha = \frac{1}{d}\ln\frac{1}{T} \tag{2}$$

where d is the thickness of AZO film.

The optical band gap of AZO film is determined through the extrapolation of linear part of the absorption edge to $\alpha = 0$ in the relationship as:

$$(\alpha h\nu)^2 = A(E_g - h\nu) \tag{3}$$

This result is basically from the intrinsic absorption of electronic transition and the value of about 3.33 eV (see Fig. 6).

The square resistance and the resistivity of ZnO:Al film are measured by four-point probe to be 667.8 Ω/□ and 0.024 Ωcm, respectively.

3.2. *I–V* characteristics

A linear *I–V* behavior between the two electrodes on the surface of ZnO:Al film indicates a good ohmic contact in Figure 7. The distance of the Al electrodes on ZnO:Al film is 1 cm. Figure 8 shows the current–voltage characteristic of

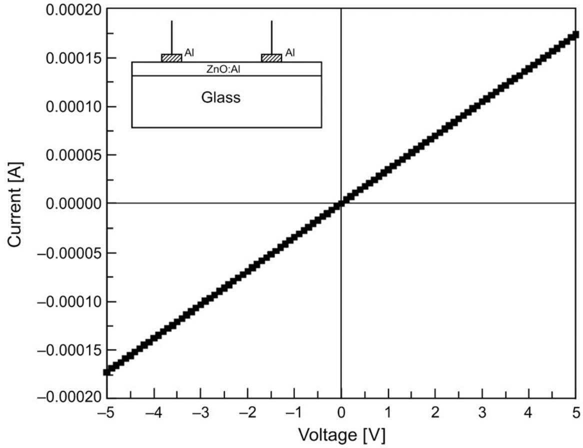

Fig. 7. *I–V* curves of two Al electrodes on AZO film.

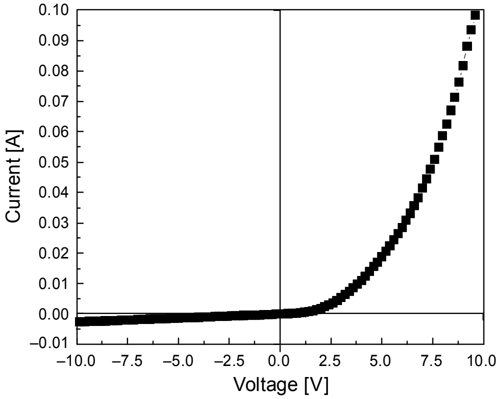

Fig. 8. *I–V* curve of the Al/AZO/SiO_2/*p*-Si/Al heterojunction device in dark.

the AZO/SiO_2/*p*-Si/Al heterojunction device measured at room temperature in the dark. Typical rectifying behavior is observed. Basing on the dark current as a function of the applied bias, the corresponding diode resistance defined as $R_D = (dI/dV)^{-1}$ [10] is derived and shown in Fig. 9. The series resistance arose from ohmic depletion plays a dominant role when the forward bias is larger than 2.5 V. When

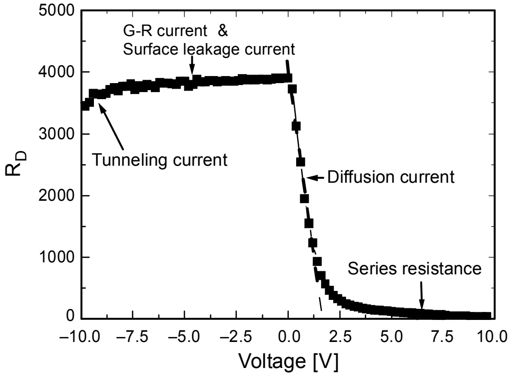

Fig. 9. The variation of diode resistance via voltage (R_D–V curve).

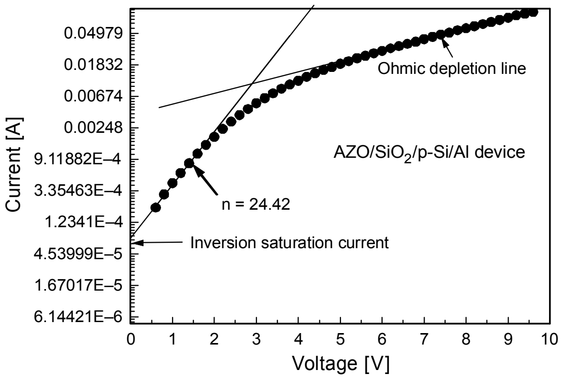

Fig. 10. The corresponding logarithmic scale in current with forward bias condition.

the voltage is between 2 V and 0 V, the resistance slightly increases as the diffusion current in the base region. When the inversion voltage increases from 0 to –5 V, the leakage current and the recombination current in the surface layers restrain the increase of the dynamic resistance, which keeps the R_D–V curve in an invariation state.

The value of the ideality factor of the heterojunction is determined from the slop of the straight line region of the forward bias log I–V characteristics (see Fig. 10). At low forward bias ($V < 2$ V), the typical values of the ideality factors and the reverse saturation current are 24.42 and 8.92×10^{-5} A, respectively. The turn-on voltage for the AZO/SiO$_2$/p-Si heterojunction is about 2.5 V. Using the standard diode equation

$$I = I_0\left(e^{\frac{qV}{nk_BT}} - 1\right)$$

where q is the electronic charge, V is the applied voltage, k_B is the Boltzmann constant, n is the ideality factor and I_0 is the saturation current [10], the values of $n = 24.42$ and $I_0 = 8.92\times10^{-5}$ A are calculated. The result of calculation (using standard diode equation) is similar to the measurement I–V curve. And the values of I_F/I_R (I_F and I_R stand for forward and reverse current, respectively) at 10 V is found to be as high as 38. It shows fairly good rectifying behavior indicating formation of a diode between AZO and p-Si.

The photo I–V characteristics were measured under illumination by low power white light (6.3 mW/cm^2) lamp and 20 W halogen lamp. The representative dark and photo I–V characteristics for the AZO/SiO$_2$/p-Si SIS heterojunction is shown Fig. 11. Typical good rectifying and photoelectric behavior were observed for the device. The dark leakage current is small, whereas its photocurrent generated under illumination is much higher. It is observed that the heterojunction exhibits a rectifying behavior in the presence of light too. Though no significant change in the current under forward bias conditions takes place after illumination, the current under reverse bias

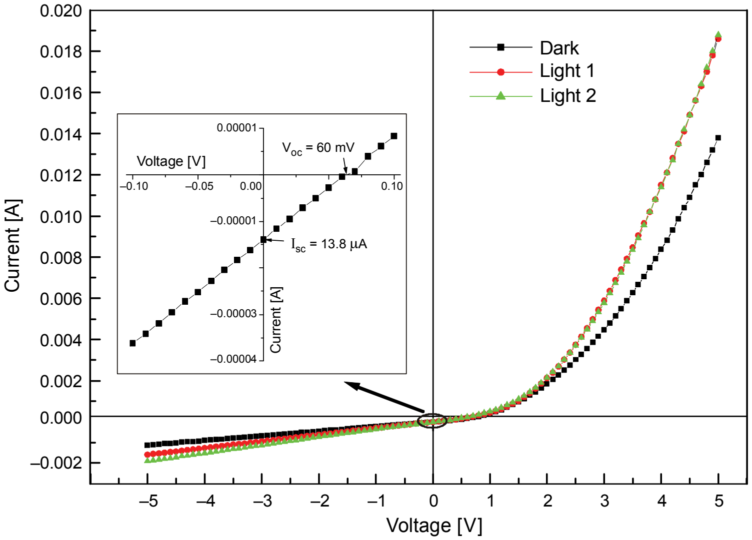

Fig. 11. *I–V* characteristic of the AZO/SiO_2/*p*-Si heterojunction in dark and in light (light 1: 6.3 mW/cm^2 white light; light 2: 20 W halogen lamp).

conditions is affected by both types of illuminations. Under reverse bias conditions photocurrent caused by the AZO surfaces exposing under illumination by low power white light lamp and 20 W halogen lamp was obviously much larger than the dark current. For example, when the reverse bias is –5 V, the dark current is only 1.13×10^{-3} A. While the reverse-bias photocurrent reach to 1.59×10^{-3} and 1.91×10^{-3} A under low power white light and halogen lamp illumination. This is generally understood that the photoelectric effect results from the light-induced electron generation at the depletion area of the *p*-Si, particularly near the heterojunction interface. Light is absorbed in the *p*-Si layer and generated electrons and holes are drifted to AZO side and Si side. So the photocurrents are consequently obtained. The mechanism behind the *I–V* characteristics can be understood by the help of the model as follows.

Since, the AZO film is highly transparent ($T > 90\%$) in the visible region, the visible light passes through AZO film and is absorbed primarily in the underlying *p*-Si, generating electron–hole pairs, responsible for the observed photocurrent under reverse bias conditions [11]. On the other hand, the UV photons are mainly absorbed in the AZO layer and the photogenerated electrons are drifted towards the positive electrode through the AZO region. Consequently, the current increases linearly as the reverse bias increases (see Fig. 11). The insert of Fig. 11 shows the AZO/SiO_2/*p*-Si heterojunction under halogen lamp illumination has great photovoltaic effect. The photovoltage of the heterojunction is 60 mV and the short circuit current is 13.8 μA.

Majority carriers are blocked from tunneling by the band gap of AZO. Tunneling can also occur via defects states at the two interfaces, we regard J_{ST} to be the dominant tunnel transition via defects in AZO-Si, where J_{ST} is the tunnel transition current.

In a device such as the SIS diode, the two semiconductors are separated by a high barrier region. The insulator is sufficiently thin (10–30 Å) so that current transport through the interface is by tunneling mechanism. Since the tunneling process is sensitive to the precipitous degree of the barrier, it is the charge transport behavior in the multi-layers semiconductor that determines the *I–V* characteristics.

The inverted *p*-type silicon surface provides a supply of minority carriers (elections) which can enter into the AZO film. The effective coupling current flows due to the interchange of the charge between the conduction and valence bands of the silicon by recombination-generation. The degree of tunneling is a function of the interface layer thickness *d*. Where open-circuit voltage is given as [12]:

$$V_{\mathrm{oc}} = \frac{nkT}{q}\left[\ln\frac{J_L}{A^* T^2} + \frac{q\phi_B}{kT} + \sqrt{q\phi_T}\, d\right] \tag{4}$$

The V_{oc} of SIS solar cell increase with interface layer thickness *d*. However, J_{sc} reduce with interface layer thickness, which make photovoltaic conversion efficiency reduce. It is reported that the best thickness of interface layer maybe 20 Å.

4. Conclusions

In summary, the microstructure, optics and electrical properties of the Al doped ZnO films, which was fabricated by RF sputtering on glass, were characterized by XRD, SEM, UV-VIS spectrophotometer, step equipment and four point probe, respectively. The average transmittance of the film is about 90% in the visible region; the band gap E_g of ZnO:Al film is 3.33 eV. The sheet resistivity and electrical (ρ) of ZnO:Al film are 667.8 Ω/□ and 0.024 Ωcm. The results show that AZO films are of good quality. AZO/SiO$_2$/*p*-Si heterojunction were successfully fabricated by RF sputtering. The *I–V* curves of device shows fairly good rectifying behaviors. The heterojunction shows great photoelectric effect under low power white light (6.3 mW/cm^2) lamp and 20 W halogen lamp illuminate. We calculated the ideality factor *n* and I_0 (the saturation current) are 24.42 and 8.92×10^{-5} A, respectively. The result of calculation (using standard diode equation) is similar to the measurement *I–V* curve. The base principle of AZO/SiO$_2$/*p*-Si heterojunction photovoltaic effect was introduced in detail.

Acknowledgments – This work was partly supported by Natural Science Foundation of China (No. 60876045), Shanghai Leading Academic Discipline Project (S30105), Innovation Foundation of Shanghai Education Committee (No. 08YZ12), R&D Foundation of SHU-SOENs PV Joint Laboratory (SS-E0700601).

References

[1] Wenas W.W., Syarif Riyadi, *Carrier transport in high-efficiency ZnO/SiO$_2$/Si solar cells*, Solar Energy Materials and Solar Cells **90**(18–19), 2006, pp. 3261–3267.

[2] Dengyuan Song, Armin G. Aberle, James Xia, *Optimisation of ZnO:Al films by change of sputter gas pressure for solar cell application*, Applied Surface Science **195**(1–4), 2002, pp. 291–296.

[3] Jaehyeong Lee, Dongjin Lee, Donggun Lim, Keajoon Yang, *Structural, electrical and optical properties of ZnO:Al films deposited on flexible organic substrates for solar cell applications*, Thin Solid Films **515**(15) ,2007, pp. 6094–6098.

[4] Bingzhi Huo, Lizhong Hu, Heqiu Zhang, *ZnO/MgO distributed Bragg reflectors*, Optica Applicata **39**(1), 2009, pp. 169–174.

[5] Ajimsha R.S., Jayaraj M.K., Kukreja L.M., *Electrical Characteristics of n-ZnO/p-Si heterojunction diodes grown by pulsed laser deposition at different oxygen pressures*, Journal of Electronic Materials **37**(5), 2008, pp. 770–775.

[6] Dengyuan Song, Neuhaus D.-H., Xia J., Aberle A.G., *Structure and characteristics of ZnO:Al/n-Si heterojunctions prepared by magnetron sputtering*, Thin Solid Films **422**(1–2), 2002, pp. 180–185.

[7] Kumar N., Kaur R., Mehra R.M., *Characterization of sol–gel derived yttrium-doped n-ZnO/p-Si heterostructure*, Materials Science-Poland **24**(1), 2006, pp. 375–383.

[8] Hui Sun, QiFeng Zhang, JinLeiWu, *Electroluminescence from ZnO nanorods with an n-ZnO/p-Si heterojunction structure*, Nanotechnology **17**(9), 2006, pp. 2271–2274.

[9] Peiliang Chen, Xiangyang Ma, Deren Yang, *Ultraviolet electroluminescence from ZnO/p-Si heterojunctions*, Journal of Applied Physics **101**(5), 2007, p. 053103

[10] HeBo, ZhongQuanMa, XuJing, ZhaoLei, ZhangNanSheng, LiFeng, ShenCheng, ShenLing, MengXiaJie, ZhouChengYue, YuZhengShan, YinYanTing, *Fabrication and photoelectrical properties of a novel violet and blue enhanced SINP silicon photovoltaic device*, Optica Applicata **39**(3), 2009, pp. 547–560.

[11] Lee J.Y., Choi Y.S., Kim J.H., Park M.O., Im S., *Optimizing n-ZnO/p-Si heterojunctions for photodiode applications*, Thin Solid Films **403–404**, 2002, pp. 553–557.

[12] Ghosh A.K., Fishman C., Feng T., *Theoretical efficiency of SnO$_2$/Si solar cells*, Journal of Applied Physics **50**(5), 1979, pp. 3454–3458.

Received March 11, 2009
in revised form June 22, 2009